

SHORT COMMUNICATION

Open Access

Morphology dependence on anions in hydrothermal synthesis of Co_3O_4

Wei-Min Zhang*, Meng Chen and Yao-Quan Jiang

Abstract

One-dimensional (1D) nanostructures of Co_3O_4 were synthesized via a mild hydrothermal route. The results of XRD, IR, and TEM revealed a phase transformation was accompanied by the replacement of NO_3^- with CO_3^{2-} throughout the hydrothermal process. The symmetric types and amount of NO_3^- and CO_3^{2-} intercalated between the brucite layers played an important role in the formation of nanowires from the hydrothermal system. The amount of CO_3^{2-} increased as the hydrothermal reaction proceeded. The substitution of CO_3^{2-} for NO_3^- led to a variation of interlayer forces thus resulted in the instability of intralayer interactions. Therefore, a shape transformation from sheets to wires occurred. Upon calcination, the shapes of precursors were preserved, and 1D nanostructures of Co_3O_4 resulted.

Keywords: One-dimensional nanostructures; Hydrothermal synthesis; Anion

Introduction

The hydrothermal system simulating the mineral formation is adapted to synthesize one dimensional (1D) nanostructured materials with high crystallinity. 1D nanostructures of Co_3O_4 have aroused great interest due to its mixed valence states [1-3]. The 1D nanostructures could be achieved by many preparative strategies [4-8]. Co_3O_4 exhibited potential application in a wide variety of fields, such as battery materials [9-11], catalysis [12,13], and magnetic materials [4,8,14]. It is now commonly known that the properties of nanomaterials strongly depend on the shape of particles, which is a dominating factor to their ultimate performance and applications [8,15-18]. In this paper, a hydrothermal pathway was carried out to investigate the controlled formation of 1D Co_3O_4 . The hydrothermal procedure was monitored combinationally by the techniques of XRD, TEM, and FT-IR in order to deeply understand the function of anions in the formation of 1D nanostructures.

Experimental

The typical preparation of 1D Co_3O_4 is described as follows: 5×10^{-3} mol $\text{Co}(\text{NO}_3)_2 \cdot 6\text{H}_2\text{O}$ and 1.25×10^{-3} mol hexamethylenetetramine (HMT) were added into the 10 mL 5×10^{-3} mol/L sodium dodecylsulfate aqueous solution

under ultrasonication. The solution was then transferred into the Teflon-lined stainless steel autoclave for hydrothermal treatment at 160°C for 6 h. The hydrothermally obtained anion-intercalated cobalt hydroxides were rinsed with deionized water and anhydrous alcohol three times and suffered calcination in air at 500°C for 6 h to produce the final products.

Thermogravimetric (TG) analysis and differential thermal analysis (DTA) were carried out in air for the precursor of Co_3O_4 with a Rigaku Thermplus TG8120 (Rigaku, Shibuya-ku, Japan) with a heating rate of $5^\circ\text{C}/\text{min}$. Powder X-ray diffraction (XRD) patterns of the samples were measured using a Rigaku γA Mini diffractometer with Cu K α radiation ($\lambda = 0.154178$ nm). The morphologies were observed by transmission electron microscopy (TEM) (obtained using a JEM-100CXII electron microscope (JEOL, Akishima-shi, Japan)) and scanning electron microscopy (SEM) (carried out by JSM-6700F). Fourier transform infrared spectra (FT-IR) of samples formed in KBr platelets were recorded with an Avatar 370 FT-IR spectrometer (Thermo Nicolet, Waltham, MA, USA) in the range of 400 to 4000/cm to investigate the crystalline form of products.

Findings

The TGA-DTA analysis for precursors suggests two steps of losing weight: the weight loss below 100°C is mainly due to dehydration of physically absorbed water, while the decomposition of NO_3^- and CO_3^{2-} ions,

* Correspondence: chm_zhangwm@ujn.edu.cn
School of Chemistry and Chemical Engineering, University of Jinan, Jiwei road,
Jinan 250022, China

together with the dehydration of OH groups between brucite layers of $\text{Co}(\text{OH})_2$ during which occurs a simultaneous conversion into spinel Co_3O_4 , contribute to the greater weight loss observed between 200°C and 500°C . Correspondingly, two endothermic peaks are shown in the DTA curve. The precursors have transformed completely into Co_3O_4 above 500°C (Figure 1).

The precondition to obtain the 1D nanostructures of Co_3O_4 is synthesizing the 1D precursor. The molar ratio of starting reactants was found as an important parameter; therefore, some experiments were carried out by varying both $\text{Co}(\text{NO}_3)_2$ and HMT amounts. Only within a very narrow range of the molar ratio of $[\text{Co}^{2+}]$ to $[(\text{CH}_2)_6\text{N}_4]$ (2:1 ~ 4:1), the wirelike precursors of cobalt basic nitrate carbonate could be obtained. The precursors and final products calcined at 500°C were further characterized by TEM and SEM techniques. A typical TEM image of Figure 2a reveals that the precursors display almost perfect 1D morphologies with widths about 100 nm. The lengths are estimated about 3 to 10 μm . Apparently, the aspect ratios of these 1D nanostructures are notably large. In addition, the precursors have proved the copiousness in quantity, and the uniformity in size distribution. The calcined products exhibit rough surfaces, as shown in Figure 2b, c, suggesting the polycrystalline feature. The energy dispersive spectrum (EDS) of the selected field, which is white framed in Figure 2c, was measured for the 500°C -calcined products, and the result displayed in Figure 2d indicates the molar ratio of Co/O equal to 0.72, in good agreement with the theoretic value of Co_3O_4 .

As shown in Figure 3, XRD, TEM, and IR techniques were employed combinationally in order to gain some insights on the function of anions in the formation of 1D Co_3O_4 .

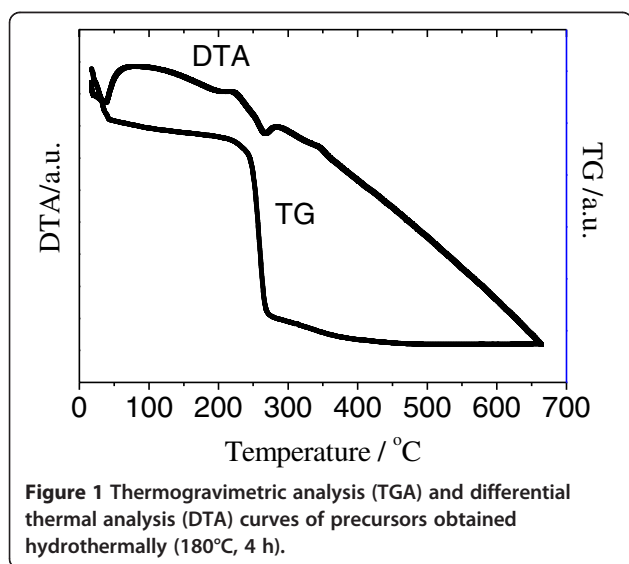
Reaction time dependence of XRD patterns for precursors exhibited a phase transformation from initial metastable

$\alpha\text{-Co}(\text{OH})_2$ to the thermodynamically stable phase, which showed a similarity with $\text{Co}(\text{CO}_3)_{0.35}\text{Cl}_{0.2}(\text{OH})_{1.1}\cdot 0.74\text{H}_2\text{O}$, implying that NO_3^- ions occupied the same position as Cl^- ions in the NO_3^- intercalated cobalt carbonate hydroxide.

The phase transformations were accompanied by the morphology alterations. As shown in Figure 3, nanosheets were obtained after 20 min of hydrothermal treatment. When the holding time was prolonged to 1 h, 1D nanostructures with the length of 2 μm coexisted with the nanosheets. After the holding time increased above 2 h, only nanowires were obtained.

FT-IR technique is an effective way to investigate the kind of anions intercalated between the $\text{Co}(\text{OH})_2$ layers. The precursor $\alpha\text{-Co}(\text{OH})_2$ taken from solution at 20 min has a large interlayer space, designated literally as a pre-hydrocalcite-like phase as confirmed by IR and XRD. Water bending mode is also found at $1,601/\text{cm}$, about $30/\text{cm}$ red shift due to strong interactions with the interlayer anions of NO_3^- and/or CO_3^{2-} . In agreement with the structural assignment, absorption peaks at $1,384$ and $839/\text{cm}$ (ν_3 and ν_2 vibration modes of NO_3^- with D_{3h} symmetry) indicate that a large number of NO_3^- anions are included [19,20]. With increasing the holding time, the intensity of the peak at $1,384/\text{cm}$ decreased obviously, and the ν_2 vibrational modes appear at $830/\text{cm}$, apparently lower than NO_3^- with D_{3h} symmetry, indicating an increment in the perturbation of the intercalated NO_3^- . Simultaneously, two peaks appear at $1,480$ and $1,312/\text{cm}$, which can be assigned to symmetric vibrational mode ($\nu_s(\text{ONO}_2)$) and asymmetric vibrations ($\nu_{as}(\text{ONO}_2)$) on monodentate nitrate, respectively. In addition, the appearance of a tiny peak at $1,312/\text{cm}$ suggests that the amount of NO_3^- is significantly reduced [19,21]. The IR spectra for sample prepared after the holding time above 2 h shows two more absorptions at $1,506$ and $1,035/\text{cm}$, which belong to the ν_3 and ν_1 vibrational modes of carbonate anions with C_{2v} symmetry. Compared with the data from Xu and Zeng [20], the two absorptions exhibited blue and red shifts, respectively. The perturbation can be attributed to stronger electrostatic interactions between the divalent CO_3^{2-} anions and the brucite-like sheets.

In summary, the probable procedure for the formation of 1D Co_3O_4 could be described as follows: initially, a large amount of NO_3^- ions intercalated between the brucite layers, adopting D_{3h} symmetry. The amount of CO_3^{2-} gradually produced by hydrolysis and oxidation of HMT increased, leading to the substitution for some of NO_3^- ions and the alteration of symmetry from D_{3h} to C_{2v} . Consequently, the modification of interlayer forces resulted in the instability of intralayer interactions, and the two-dimensional nanosheets eventually transformed to 1D nanostructures. The morphology was preserved in calcination to produce 1D Co_3O_4 .



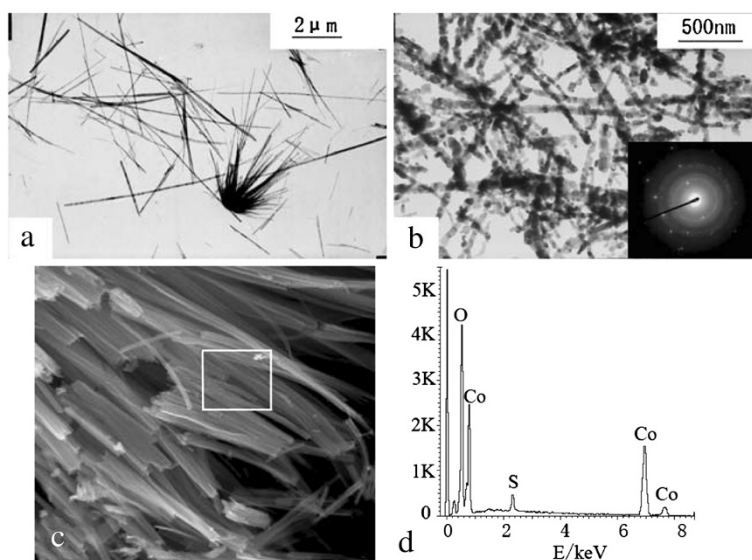


Figure 2 The morphology of the precursor (a), the calcined products (b and c), and EDS (d). SAED of the calcined products is inset in (b), and EDS results white framed in (c) are also exhibited in (d).

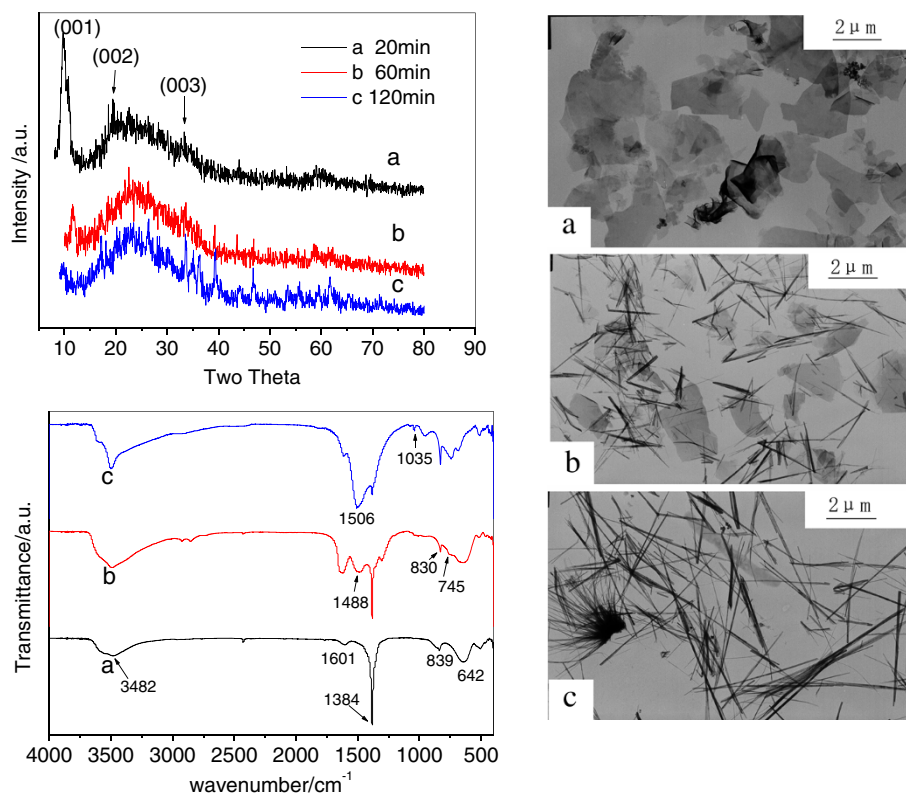


Figure 3 Temporal evolution of XRD patterns, TEM images, and IR spectrum. For precursors taken out of the autoclave at different stages of hydrothermal treatment: (a) 20, (b) 60, and (c) 120 min.

Competing interests

The authors declare that they have no competing interests.

Authors' contributions

WMZ, as the corresponding author, instructed the other two authors to carry out the experiments and drafted the manuscript. MC synthesized the samples and contributed a lot in phase analysis of samples using techniques of XRD and TEM. YQJ provided his contributions in the IR analysis. All authors read and approved the final manuscript.

Received: 4 July 2012 Accepted: 30 April 2013

Published: 15 July 2013

References

1. Lakshmi, BB, Patrisi, CJ, Martin, CR: Sol-gel template synthesis of semiconductor oxide micro- and nanostructures. *Chem. Mater.* **9**, 2544–2550 (1997)
2. Liu, Y, Wang, G, Xu, C, et al.: Fabrication of Co_3O_4 nanorods by calcination of precursor powders prepared in a novel inverse microemulsion. *Chem. Commun.* 1486–1487 (2002)
3. Wang, D, Caruso, RA, Caruso, F: Synthesis of macroporous titania and inorganic composite materials from coated colloidal spheres - A novel route to tune pore morphology. *Chem. Mater.* **13**, 364–371 (2001)
4. Meher, SK, Rao, GR: Ultra-layered Co_3O_4 for high performance supercapacitor applications. *J. Phys. Chem. C* **115**, 25543–25556 (2011)
5. Wei, C, Nan, Z: Effects of experimental conditions on one-dimensional single-crystal nanostructure of $\beta\text{-FeOOH}$. *Mater. Chem. Phys.* **127**, 220–226 (2011)
6. Chen, N, Huang, C, Yang, W, et al.: Growth control for architecture molecular conductor of low dimension nanostructures. *J. Phys. Chem. C* **114**, 12982–12986 (2010)
7. Kar, S, Pal, BN, Chaudhuri, S, et al.: One-Dimensional ZnO nanostructure arrays: Synthesis and characterization. *J. Phys. Chem. B* **110**, 4605–4611 (2006)
8. Wang, G, Shen, X, Horvat, J, et al.: Hydrothermal synthesis and optical, magnetic, and supercapacitive properties of nanoporous cobalt oxide nanorods. *J. Phys. Chem. C* **113**, 4357–4361 (2009)
9. Wang, B, Wang, Y, Park, J, et al.: In situ synthesis of Co_3O_4 /graphene nanocomposite material for lithium-ion batteries and supercapacitors with high capacity and supercapacitance. *J. Alloys Compd.* **509**, 7778–7783 (2011)
10. Yao, X, Xin, X, Zhang, Y, et al.: Co_3O_4 nanowires as high capacity anode materials for lithium ion batteries. *J. Alloys Compd.* **521**, 95–100 (2012)
11. Li, L, Wang, Y, Wang, Y, et al.: Mesoporous nano- Co_3O_4 : A potential negative electrode material for alkaline secondary battery. *J. Power. Sources* **196**, 10758–10761 (2011)
12. Cui, Y, Wen, Z, Sun, S, et al.: Mesoporous Co_3O_4 with different porosities as catalysts for the lithium–oxygen cell. *Solid State Ionics Solid State Ion.* **225**, 598–603 (2012)
13. Asano, K, Ohnishi, C, Iwamoto, S, et al.: Potassium-doped Co_3O_4 catalyst for direct decomposition of N_2O . *Appl. Catal. B* **78**, 242–249 (2008)
14. Nethravathi, C, Sen, S, Ravishankar, N, et al.: Ferrimagnetic nanogranular Co_3O_4 through solvothermal Decomposition of colloidal dispersed monolayers of α -cobalt hydroxide. *J. Phys. Chem. B* **109**, 11468–11472 (2005)
15. Geng, B, Zhan, F, Fang, C, et al.: A facile coordination compound precursor route to controlled synthesis of Co_3O_4 nanostructures and their room-temperature gas sensing properties. *J. Mater. Chem.* **18**, 4977–4984 (2008)
16. Jia, Z, Wang, Q, Ren, D, et al.: Fabrication of one-dimensional mesoporous $\alpha\text{-Fe}_2\text{O}_3$ nanostructure via self-sacrificial template and its enhanced Cr(VI) adsorption capacity. *Appl. Surf. Sci.* **264**, 255–260 (2013)
17. Luo, Z, Yin, S, Wang, K, et al.: Synthesis of one-dimensional $\beta\text{-Ni}(\text{OH})_2$ nanostructure and their application as nonenzymatic glucose sensors. *Mater. Chem. Phys.* **132**, 387–394 (2012)
18. Song, Q, John Zhang, Z: Shape control and associated magnetic properties of spinel cobalt ferrite nanocrystals. *J. Am. Chem. Soc.* **126**, 6164–6168 (2004)
19. Xu, ZP, Zeng, HC: Interconversion of brucite-like and hydroxalite-like phases in cobalt hydroxide compounds. *Chem. Mater.* **11**, 67–74 (1999)

20. Xu, ZP, Zeng, HC: Thermal evolution of cobalt hydroxides: a comparative study of their various structural phases. *J. Mater. Chem.* **8**, 2499–2506 (1998)
21. Schraml-Marth, M, Wokaun, A, Baikert, A: Surface structure of crystalline and amorphous chromia catalysts for the selective catalytic reduction of nitric oxide IV. Diffuse reflectance FTIR study of NO adsorption and reaction. *J. Catal.* **138**, 306–321 (1992)

doi:10.1186/2228-5326-3-44

Cite this article as: Zhang et al.: Morphology dependence on anions in hydrothermal synthesis of Co_3O_4 . *International Nano Letters* 2013 **3**:44.

Submit your manuscript to a SpringerOpen[®] journal and benefit from:

- Convenient online submission
- Rigorous peer review
- Immediate publication on acceptance
- Open access: articles freely available online
- High visibility within the field
- Retaining the copyright to your article

Submit your next manuscript at ► springeropen.com